An approach to produce thousands of single-chain antibody variants on a SPR biosensor chip for measuring target binding kinetics and for deep characterization of antibody paratopes

Rebecca L. Cook, William Martelly, Chidozie V. Agu, Lydia R. Gushgari, Salvador Moreno, Sailaja Kesiraju, Mukilan Mohan, Bharath Takulapalli

Abstract

Drug discovery continues to face a staggering 90% failure rate, with many setbacks occurring during late-stage clinical trials. To address this challenge, there is an increasing focus on developing and evaluating new technologies to enhance the "design" and "test" phases of antibody-based drugs (e.g., monoclonal antibodies, bispecifics, CAR-T therapies, ADCs) and biologics during early preclinical development, with the goal of identifying lead molecules with a higher likelihood of clinical success. Artificial intelligence (AI) is becoming an indispensable tool in this domain, both for improving molecules identified through traditional approaches and for the de novo design of novel therapeutics. However, critical bottlenecks persist in the "build" and "test" phases of AI-designed antibodies and protein binders, impeding early preclinical evaluation. While AI models can rapidly generate thousands to millions of putative drug designs, technological and cost limitations mean that only a few dozen candidates are typically produced and tested. Drug developers often face a tradeoff between ultra-high-throughput wet lab methods that provide binary yes/no binding data and biophysical methods that offer detailed characterization of a limited number of drug-target pairs. To address these bottlenecks, we previously reported the development of the Sensor-integrated Proteome On Chip (SPOC®) platform, which enables the production and capture-purification of 1,000 – 2,400 folded proteins directly onto a surface plasmon resonance (SPR) biosensor chip for measuring kinetic binding rates with picomolar affinity resolution. In this study, we extend the SPOC technology to the expression of single-chain antibodies (sc-antibodies), specifically scFv and VHH constructs. We demonstrate that these constructs are capture-purified at high levels on SPR biosensors and retain functionality as shown by the binding specificity to their respective target antigens, with affinities comparable to those reported in the literature. SPOC outputs comprehensive kinetic data including quantitative binding (R_{max}), on-rate (k_a), off-rate (k_d), affinity (K_D), and half-life ($t_{1/2}$), for each of thousands of on-chip sc-antibodies. Additionally, we present a case study showcasing single amino acid mutational scan of the complementarity-determining regions (CDRs) of a HER2 VHH (nanobody) paratope. Using 92 unique mutated variants from four different amino acid substitutions, we pinpoint critical residues within the paratope that could further enhance binding affinity. This study serves as a demonstration of a novel high-throughput approach for biophysical screening of hundreds to thousands of single chain antibody sequences in a single assay, generating high affinity resolution kinetic data to support antibody discovery and AI-enabled pipelines.

Introduction

Biopharmaceutical companies invest billions of dollars annually in developing new drugs to prevent and treat diseases, yet only about 10% of drug candidates that enter development pipelines and clinical trials ultimately receive regulatory approval[1,2]. The majority of failures are attributed to inadequate efficacy and/or safety, which are often linked to the on- and off-target binding properties of drug molecules. As a result, there is a renewed emphasis on designing new molecular entities (NMEs), particularly biologics, that exhibit high affinity, specificity, and selectivity to their intended targets in early preclinical phase, towards furthering the candidates with improved profiles along the development pipelines. Currently, deep characterization of binding kinetics is typically performed during the lead selection process, and safety assessments are often conducted during costly in vivo animal studies (**Figure 1)**. To improve success rates, it is critical to assess kinetic binding and safety profiles earlier in the preclinical workflow—ideally in the design phase—while striving to maintain a broader diversity of lead candidates. Achieving this requires new or improved methods to accelerate the design, build, and test cycles, for iterative improvement and down selection of most optimal lead candidates. Such advancements could significantly enhance clinical success rates, saving biopharma hundreds of millions of dollars annually, and expediting the delivery of new and improved therapies to patients.

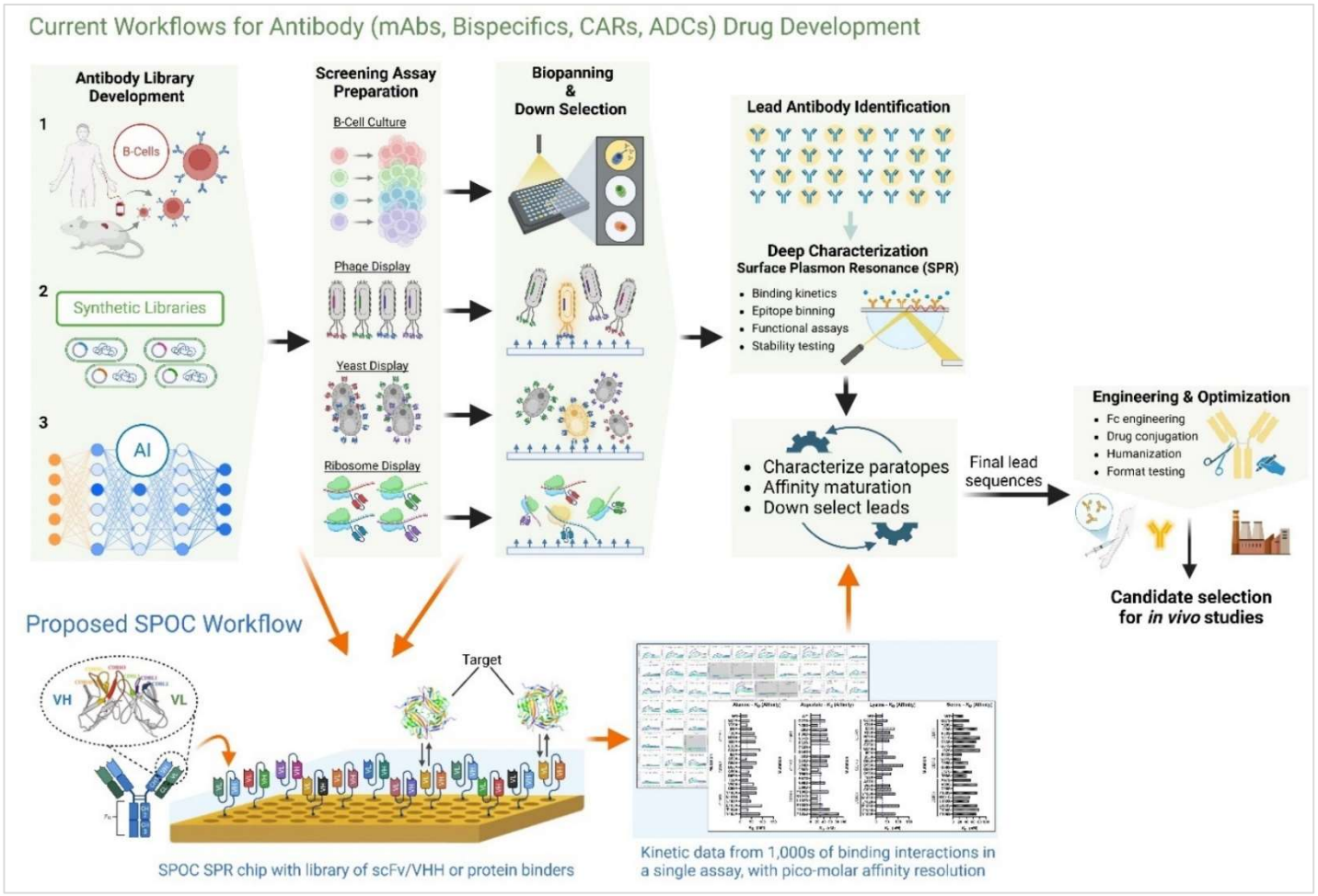

Figure 1: Schematic of current antibody drug development approaches and the proposed integration of SPOC into these workflows. Antibody sequence libraries have traditionally been harvested from 1) B-cells collected from naïve or immunized animals or convalescent patient serum, 2) derived from synthetic cDNA constructs, and 3) increasingly from generative artificial intelligence (AI) applied to in silico design of biologics. These inputs feed into a plurality of screening assays. Isolated B-cells are cultured, and secreted antibodies are assayed for clones that bind target antigen, which are subsequently sequenced. For inputs where sequences are already known, as after B-cell sequencing or for synthetic libraries or AI, various display technologies (phage,

yeast, and ribosomes) can be directly employed whereby these cell-lines or ribosomes are applied to synthesize millions of sc-antibody variants for downstream panning against target antigens, and sequencing of the binders. After initial panning assays that isolate and identify the binders, deeper characterization is performed to assess the functional activity of lead candidates and interrogate their target binding mechanisms and kinetics with the use of label-free techniques such as surface plasmon resonance (SPR). These workflows involve additional paratope characterization steps and affinity maturation cycles, with the objective of down-selecting final lead sequences that are further engineered and optimized for efficacy and safety, prior to initiating humanization, Fc engineering and in vivo studies. We propose integrating SPOC platform into current workflows (lower part of the figure), wherein variable domain sequences derived from libraries can be directly leveraged for cell-free production and capture of sc-antibody libraries on SPR biosensor chips. SPOC facilitates measuring binding kinetics of all binders for down-selection by producing rich data, enabling deep characterization of the paratopes of lead antibodies and antibody affinity maturation cycles towards selecting optimally engineered lead candidates.

Machine learning (ML) and generative artificial intelligence (AI) are revolutionizing drug development, with several AI-designed drug molecules now advancing to clinical trials, signaling a transformative era in drug design and discovery. Current ML methods for drug discovery leverage iterative design-build-test-learn (DBTL) cycles to create high-affinity binders for drug targets (**Figure 2**). AI models can produce millions of initial candidate binders in a single 'design-phase' run, that are reduced to a few thousand by *in-silico* binding predictions. However, the subsequent build (synthesis) and test phases remain major bottlenecks due to their ex-silico nature, which is both capital and time-intensive. This capability-gap limits the scalability of DBTL cycles, as only a fraction of the candidates can be synthesized and tested experimentally. While powerful, AI models for protein design and binding analysis rely heavily on high-quality, large-scale wet lab data sets to train and refine their predictions, and are thus only as good as the real-world data they are trained on. New wet lab technologies are needed not only to generate data at scale for initial training but also for testing and improvement of antibody and protein binders through iterative cycles.

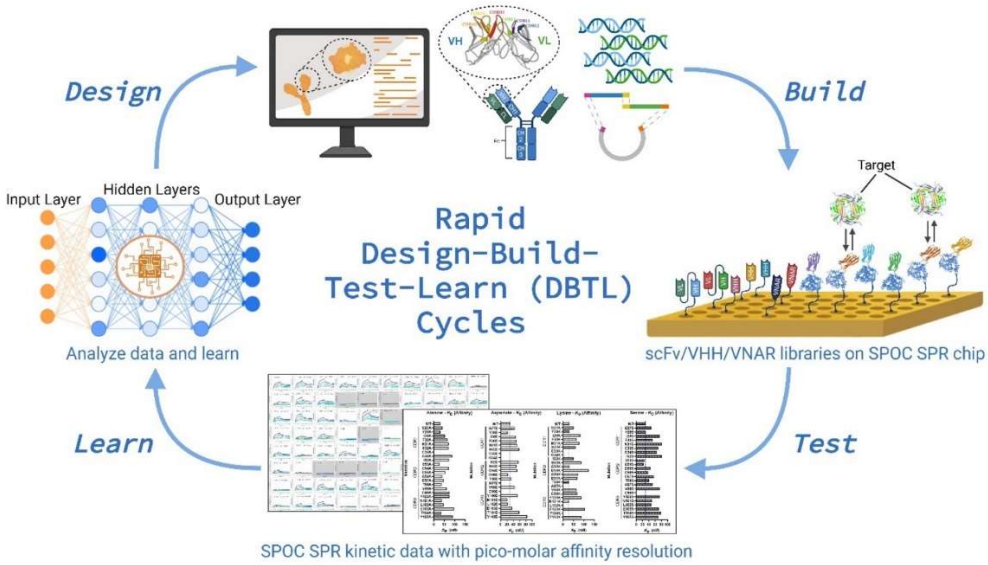

Figure 2: **Schematic of SPOC assay integration into iterative AI-driven discovery workflows.** Using inputs from trained AI models, sequences for numerous antibody sequences or protein binders (or other target-binding scaffolds and protein designs) can be cloned into cell-free expression vectors to rapidly build sc-antibody or protein libraries on SPOC SPR chips that can be screened with the desired target(s) to yield a wealth of detailed kinetic binding data. These rich kinetic datasets can then feed back into AI models providing additional training data to learn from, enabling the further refinement of AI-designed binders.

For conventional and AI-driven drug discovery workflows, experimental testing methods typically balance between ultra-high-throughput assays, which offer binary yes/no binding data, and more comprehensive techniques that yield detailed kinetic and biophysical data but can only accommodate a limited set of binders. Due to the cost-prohibitive nature of synthesizing and testing thousands of candidates, biophysical characterization is often limited to a few dozen lead molecules, representing a significant forced-reduction in sequence diversity. For example, interrogating binding characteristics using techniques such as surface plasmon resonance (SPR) in a high throughput manner is limited both by the limitations in the build (synthesis) phase as well as requirement for significant quantities of each drug candidate for sensor deposition and testing, limiting throughput. Moreover, ultra-high-throughput screening methods, such as phage and yeast display, often produce lead candidates with redundant sequences, reducing the diversity of final selections. The application of next-generation sequencing (NGS) has demonstrated its ability to identify rare clones missed by traditional pull-down assays, highlighting the inadequacy of current methods in capturing sequence diversity comprehensively[3–6]. These limitations underscore the need for novel high-throughput wet lab assays capable of producing diverse, high-quality data to better inform candidate selection and advance the integration of AI into drug development pipelines.

The class of antibody therapeutics and biologics has undergone significant innovation over the past two to three decades, driving the development of newer therapeutic modalities and yielding highly effective drugs, even as we enter the new age of AI-driven drug design. Following the success of full-length antibody therapeutics such as trastuzumab (Herceptin), bevacizumab (Avastin), and adalimumab (Humira) at the turn of the century, the therapeutic landscape has expanded dramatically to include a diverse and powerful array of novel single-chain antibody derivatives. These include single-chain antibody formats such as single-chain variable fragments (scFvs), single variable domain of heavy-chain antibodies (VHH, also known as nanobodies, which is a trademark of Ablynx N.V), and shark-derived variable new antigen receptors (VNARs); this is in addition to antibody mimetics such as designed ankyrin repeat proteins (DARPins), and a diverse class of AI designed protein binders. Single-chain antibodies, in particular, offer several advantages due to their smaller size, which often enhances tissue penetration and have fewer functional components outside of the antigen binding region compared to most mammalian antibodies, potentially lowering immunogenicity. These compact structures are also easier to produce using a range of expression systems, including yeast and bacterial platforms such as *E. coli*.

Nanobodies, which are derived from the antigen-binding region of specialized single-domain antibodies found in camelids (such as llamas, camels, and alpacas), hold immense promise for current and future clinical applications. These compact molecules, ranging from 12 to 15 kDa in size, consist of a single immunoglobulin domain that exhibits high-affinity binding (nM to pM range) even though it lacks a light chain. The small size and unique structure of nanobodies enable them to access cryptic antigens that conventional full-length antibodies cannot reach. Additionally, in certain modalities, their compact nature can facilitate cellular uptake into the cytoplasm, allowing them to target intracellular antigens[7]. Like the variable regions of IgG molecules, nanobodies possess three complementarity-determining regions (CDRs) that form the antigen-binding site (paratope). However, unlike IgGs, nanobodies are more thermostable, less prone to aggregation, and exhibit a shorter half-life—though the latter can be extended through conjugation with specific proteins. The clinical potential of nanobodies was underscored in 2018 with the FDA approval of Caplacizumab, the first nanobody-based drug for humans, used to treat acquired thrombotic thrombocytopenic purpura[8]. Caplacizumab demonstrated not only therapeutic efficacy but also low immunogenicity, highlighting its safety for clinical use. Since then, nanobody-based therapies have rapidly expanded with a CAR-T cell therapy (Ciltacabtagene autoleucel) incorporating a nanobody-based antigen receptor that was approved in the US and EU in 2022, a nanobody for treating solid tumors (Envafolimab) approved in China in 2021, and Ozoralizumab, a nanobody to treat rheumatoid arthritis approved in Japan in 2022[9–11]. Numerous others nanobody based therapies are in clinical trials for treatment of infectious disease, autoimmune disease, and cancer.

Given the therapeutic promise of sc-antibodies and protein binders, drug developers are increasingly focusing on engineering these molecules to address previously encountered challenges related to affinity, specificity, selectivity, and tissue distribution observed in earlier generations of antibody drugs. These efforts aim to enable

access to previously obscure targets or specific epitopes, significantly expanding therapeutic possibilities. The growing popularity of sc-antibody drug discovery is evident from the proliferation of commercially available synthetic libraries, including fully naïve libraries, designed for rapid target screening and high throughput binder identification. AI-driven engineering of sc-antibodies and protein binders offers the potential to further accelerate the development of new therapies by optimizing paratopes for specific clinical targets. However, realizing this potential requires the development of new wet lab techniques capable of high-throughput, deep characterization of these engineered molecules. Such techniques are essential for rapid testing, analysis, and iterative improvement cycles to identify leads with very high affinity (or affinity optimized for specific therapeutic modalities), high specificity and selectivity, ensuring their readiness for preclinical and clinical testing.

As part of the design-build-test-learn (DBTL) cycles in drug development, affinity maturation campaigns are frequently undertaken to iteratively enhance the binding properties of identified binders and lead candidates. The initial step in this process involves deep characterization of the sc-antibody paratopes. This is typically achieved through comprehensive degenerate mutagenesis or computationally driven designer mutations introduced into the CDRs, linkers, and/or scaffold regions. Again, current limitations in the "build" and "test" phases significantly constrain this process. The high cost of producing the library of mutants designed by AI limits the number of sequences that can be experimentally tested for lead selection. As a result, mutations are often restricted to specific substitutions, such as alanine scanning. This narrow approach risks overlooking critical paratope residues essential for binding or alternative amino acid substitutions that cumulatively could significantly enhance binding affinity, potentially missing opportunities to achieve sub-picomolar binders and to develop "best-in-class" drug candidates. The limitations of current technologies in generating and testing sufficient sequence diversity can result in suboptimal lead candidates, undermining the potential of affinity maturation campaigns. To address these challenges and bridge the gaps in the "build" and "test" phases, we propose leveraging the previously reported Sensor-integrated Proteome On Chip (SPOC®) platform[12].

The SPOC technology offers a transformative solution for high-throughput deep kinetic characterization of sc-antibody (e.g., scFv and VHH) variants, enabling the production of SPR biosensor chips with hundreds to thousands of unique sc-antibody drug candidates produced and captured on chip. The platform allows for direct and simultaneous high-resolution kinetic measurements of analyte binding (e.g., antigen targets in solution) across the entire on-chip scFv or VHH library in a single assay. To address the cost and scalability challenges of the "build" phase, the SPOC platform utilizes nanoliter-scale cell-free protein expression within high-density nanowells. This approach facilitates the production of thousands of properly folded proteins in discretely separated and isolated nanowells, within a 1.5-square-centimeter area, which are then directly capture-purified onto SPR biosensor chips. The SPOC system enables the characterization of binding interactions for up to 1000–2400 sc-antibody variants against their antigen target or alternative analytes of choice (e.g., potential off-targets).

The sc-antibodies are covalently captured on the SPR biosensor chip, allowing for enhanced stability and offering the potential for multiple rounds of regeneration and follow-on assays. This feature ensures that a single chip may be reused for collecting replicate data, further improving cost-efficiency and throughput in the characterization and validation processes. Importantly, the SPOC workflow only requires the DNA sequence library encoding the sc-antibodies or protein binders, eliminating the need for expression and purification of proteins. By leveraging plasmid or linear DNA and cell-free expression systems to convert sc-antibody gene/DNA libraries into protein libraries, the SPOC platform dramatically reduces the time and cost associated with obtaining high affinity resolution SPR kinetic data which provides a wealth of information about the binding characteristics of each sc-antibody on the sensor, including (R_{max}), on-rate (k_a), off-rate (k_d), affinity (K_D), and half-life ($t_{1/2}$). Compared to traditional recombinant production approaches, this innovation accelerates the testing and validation process, making it feasible to generate the large-scale, high-quality wet lab data required to train AI models for better prediction accuracies. SPOC technology thus bridges critical gaps in the "build" and "test" phases, enabling rapid, cost-effective, and scalable characterization of antibody libraries to support state of the art drug discovery pipelines. In this study, we demonstrate the application of SPOC technology for the production and analysis of sc-

antibodies for the first time. As a use case, we analyze the CDRs of a well-characterized HER2 nanobody utilizing single amino acid mutational scanning to identify key residues critical for optimizing binding affinity and function.

Methods

Materials and Reagents

Halo-PEG(2)-NH2*HCl (RL-3680) was sourced from Iris Biotech GmBH through Peptide Solutions, LLC. Rabbit anti-HaloTag (G9281) and TMR-Halo Ligand (G8251) were obtained from Promega. Mouse anti-HaloTag (#28a8) and Halo VHH (#ot) was obtained from ProteinTech.

ScFv and VHH antigen targets were sourced as follows: recombinant human TNF alpha (TNFα), BioLegend #570102; recombinant human IL-6, Biolegend #570802; recombinant human HER2 (AA 23-653), Acro Biosystems HE2-H5225; recombinant human CEACAM-5 (CEA), R&D Systems 4128-CM; recombinant human EGFR-Fc, R&D Systems 344-ER-050; recombinant human p53, Active Motif 81091.

Detection antibodies were sourced as follows: Alexa Fluor® 647 Rat anti-human IL-6, Biolegend 501123; Mouse anti-human TNF-α Antibody, BioLegend 502901; Human anti-HER2 (Trastuzumab), Selleck Chemicals A2007; Human anti-CEA (Tusamitamab), Selleck Chemicals A2544; Mouse anti-p53, Sigma P6874; Goat anti-rabbit-Cy3 (Jackson ImmunoResearch 111-165-003), Goat anti-mouse-Cy3 (Jackson ImmunoResearch 115-165-062), Goat anti-Human IgG-Cy3, Jackson ImmunoResearch 109-165-098.

Identification and construction of single-chain antibody sequences for testing

For proper evaluation of single chain antibodies on the SPOC platform, we chose to test sequences which were well characterized and reported in literature or were otherwise publicly available, such as FDA approved drugs. Sequences were identified using the ExPasy ABCD (AntiBodies Chemically Defined) Database (https://web.expasy.org/abcd/), the International Immunogenetics Information System (IMGT, https://www.imgt.org/) , and associated PubMed resources.

Sequences were designed and codon optimized for cell-free expression using a IVTT *E. coli*-based kit. These constructs maintain a T7 Promoter-5' UTR-Gene-HaloTag-T7 Terminator structure. The antibody sequences were derived from literature and converted to scFv format by extracting the VH and VL sequences and separating them with a $(Gly_4Ser)_3$ linker. A $(Gly_4Ser)_3$ linker was also placed between the scFv sequence and a C-terminal HaloTag. All DNA was synthesized by Twist Biosciences or Alta Biotech.

The HaloTag was chosen as the fusion tag of choice for our studies due to the covalent bond it forms with its chloroalkane ligand (Halo ligand) that is immobilized on the SPR biosensor surface. The HaloTag is derived from a halogenase enzyme; because the HaloTag protein contains an active site capable of catalyzing a covalent bond between the enzyme's active site and a haloalkane when it is properly folded, the use of the HaloTag on the C-terminus of our constructs provides additional confidence that the linker-fused protein of interest is expressed in frame and is properly folded. The underlying rationale is that if the protein-Halo construct is covalently linked to a surface functionalized with chloroalkane (Halo ligand), the HaloTag itself must be folded properly to be enzymatically active for covalent bond formation with the chloroalkane on the sensor surface, and thus, the N-terminal fusion protein is more likely to have undergone proper folding as well.

In-tube expression of scFvs and nanobodies for validation studies

E. coli constructs were expressed according to the standard protocol for 6 hours at 37° C, and stored overnight at 4° C prior to assay the next day. For these constructs, a final DNA concentration of 10 nM was used and all reactions were performed in a 96-well PCR plate.

Validation of protein expression and molecular weight via SDS-PAGE

All HaloTagged products from *E. coli* expression reactions were visualized in-gel via tetramethylrhodamine (TMR) fluorescent labeling. Briefly, each cell-free expression reaction was incubated with TMR-Halo ligand in a 1:1:5 ratio of undiluted expression reaction:50 nM TMR-Halo ligand (Promega):PBS for 15 minutes at room temperature in the dark. Labeling with TMR-Halo ligand prior to denaturation for SDS-PAGE was critical to not destroy the Halo ligand active site/allow the covalent modification of the HaloTagged protein with TMR-Halo. Labeled samples were then prepared in both reducing and non-reducing conditions using Bolt LDS Sample Buffer (Invitrogen) and Bolt Sample Reducing Agent for reducing conditions (Invitrogen), incubated for 5 minutes at 95° C, and loaded into a Bolt Bis-Tris 4-12% gels (Invitrogen). Gels were visualized using the fluorescent protein gel function on a Thermo iBright system (Thermo Fisher Scientific).

Manual testing of single chain antibody binding

To analyze the ability of single chain antibodies to bind to their intended target and to measure any off-target binding prior to automated SPR analysis, scFvs and VHH were first tested manually in a multiplexed sandwich assay on glass slides. Glass slides with a hydrogel coating (Schott Nexterion Slide H) were first functionalized with 4 mM Halo ligand and then blocked with Superblock-TBS (Thermo Fisher Scientific). The slides were rinsed with diH2O and dried under a nitrogen stream, then affixed with a 64-well Flexwell incubation chamber (Grace Bio-Labs). 5 µL of HaloTagged scFv or VHH cell-free expression reaction was added to each well, followed by 15 µL PBST (PBS, pH 7.4, 0.2% Tween-20), and incubated for 1 h at room temperature on a rocker. Enough wells were filled to test each antigen against each scFv or VHH, regardless of specificity, to enable measurement of non-specific binding of antigen.

Wells were then washed 3 times with PBST, and the target antigen was added at a concentration of 50 nM for most, or 1:20,000 for IgG/IgM-depleted serum (Pel-Freez) for detection of human serum albumin. Negative controls were incubated with PBST instead of antigen. Antigen was incubated for 1 hour at room temperature on a rocker, then washed 3 times with PBST. Detection of antigen bound to scFvs or VHHs was done by incubating with a primary antibody against the antigen for 1 hour at room temperature on a rocker using a 1:500 dilution in 5% milk in PBST, then washed 3 times in PBST. For any primary antibodies that were not fluorescently labeled, a fluorescently labeled secondary antibody was incubated in the well for 30 minutes using a 1:500 dilution in 5% milk/PBST, then washed 3 times with PBST. One set of wells was also incubated with anti-HaloTag antibody and corresponding secondary antibody to measure total HaloTagged protein bound in the well. Prior to imaging, all slides were gently rinsed with diH2O and dried under a nitrogen stream.

Slides were imaged with an Innoscan 910AL (Innopsys) using sequential scanning of the 635 nm and 532 nm channels and Mapix software. Quantification was performed using a custom-made GAL file built for the 64-well Flexwell layout, in combination with the Mapix quantification feature. Background signal was subtracted from each well, then normalized to anti-HaloTag signal.

Preparation and printing of nanowell slides

Silicon nanowell slides (1” x 3”) containing 11,280 individual nanowells were prepared as previously described for DNA printing[12]. Briefly, slides were treated with oxygen plasma for 2 minutes at 50 W followed by vapor phase coating with APTES ((3-Aminopropyl)-triethoxysilane) and curing for 1 hour at 100° C. DNA was diluted to 100 ng/µL in nuclease-free H2O. Printing of DNA into nanowells was performed with assistance from Engineering Arts, LLC using a Rainmaker 3 piezo-based printer (Bio-Dot) following printing of a print mix composed of bis(sulfosuccinimidyl)suberate (BS3, Thermo Fisher Scientific) and bovine serum albumin (BSA) into each individual well. Printed slides were allowed to dry in the humidified printing chamber for 15 minutes prior to removal, then stored in desiccating conditions at room temperature prior to assay.

Capture of protein onto SPR biosensors

To enable capture of thousands of unique proteins onto planar substrates, SPOC Proteomics designed and built an in-house automated system termed Protein Nano Factory (PNF, previously referred to as AutoCap). The PNF

system is capable of introducing cell-free expression lysate into each individual nanowell, incubating the slide for proper expression of protein within each nanowell, and transferring the expressed HaloTagged protein to a planar substrate (glass or biosensor) press-sealed against the nanowell slide[12]. The result is a planar substrate covered in discrete, circular spots each containing a pure protein uniquely expressed in each well, with no discernable cross binding between spots[12] . Xantec HC30M gold slides were used as the planar substrate for SPR biosensor production. Gold biosensor slides were first prepared for protein capture by activating for 10 minutes with a 1:1:1 solution of 0.4M N-(3-dimethylaminopropyl)-N-ethylcarbodiimide (EDC), 0.1 M N-hydroxysuccinimide (NHS), and 0.1 M 2-(N-morpholino) ethanesulfonic acid, pH 5.5 (MES), followed by water rinse and drying with a steady nitrogen stream. Slides were then functionalized with 1 mg/mL Halo-PEG(2)-NH2 overnight at room temperature (Iris Biotech; RL-3680) . Any free NHS groups were quenched using 0.5 M ethanolamine, pH 8.5, then gently washed with diH2O and dried under nitrogen prior to loading onto the AutoCap instrument. Printed nanowell slides were prepared for the AutoCap instrument by blocking in SuperBlock-TBS for 30 minutes, then washed with diH2O and dried under nitrogen.

Following loading of the slides into individual chambers on the PNF system, the chambers were vacuumed and followed with injection of 500 µL of cell-free expression lysate. The nanowell and biosensor slides were then automatically pressed together following injection, isolating each individual nanowell with cell-free expression lysate and DNA to enable protein expression and immediate capture onto the biosensor. The chambers were incubated for 6 hours at 37° C prior to slide removal and immediate rinsing with PBST to remove unbound protein and lysate. SPR biosensors were either loaded immediately onto a custom Carterra LSA^{XT} SPR biosensing instrument for equilibration and assay, or stored in 50% glycerol at -20° C for later assay.

Label-free and multiplex detection of in-solution analytes binding to single chain antibody molecules captured on SPR biosensors

Biosensors were rinsed with PBS followed by water prior to loading onto the Carterra SPR instrument compatible prism cartridge using 10-15 µL of refractive index-matching mounting oil (Cargille). The sensor was then loaded into a custom Carterra SPR instrument and equilibrated overnight in fresh, filtered, and degassed SPR buffer (1X PBS, 0.2% BSA, 0.05% Tween-20, pH 7.2). On this custom instrument, the individual protein spots are visible and can be assigned identifiers using regions of interest (ROI) prior to analyte screening. For validation of protein capture via mouse anti-HaloTag antibody binding, an association time of 6 min and dissociation time of 12 minutes was used. For analysis of analytes binding to single chain antibodies, 15-60 minutes association and 2 minutes dissociation was used. 15 minute association and 20 minute dissociation times were used for calculating affinity constants and other kinetic parameters for the initial affinity study with TNFα VHH and HER2 VHH. 20 minute association and 30 minute dissociation times were used for calculating affinity constants for measuring kinetics in the HER2 VHH mutation scan.

Analysis of SPR biosensor data

Data collected from the custom Carterra LSA^{XT} SPR biosensing instrument was analyzed using Kinetics analysis software (Carterra). Raw data was y-aligned and double referenced against the leading running buffer only blank injection and no ligand control spots present on the sensor. Excessive spikes were filtered using standard settings (height = 7, width = 9). Processed, double-referenced data was then globally fit with a 1:1 Langmuir binding model to extract kinetic binding rates and other associated metrics [on-rate (k_a), off-rate (k_d), affinity (K_D), R_{max}, and half-life ($t_{1/2}$)]. Mutants with <10% of the maximum signal observed for the highest binder after injection of 400 nM HER2 ECD were considered non-binders for purposes of analysis. Visualization of mutants was performed using PyMol version 3.1.3 based on PDB structure 5MY6[13].

Results

Expression validation of scFv and VHH constructs

All scFvs and VHHs (**Table 1**) were designed as C-terminal HaloTag fusion proteins for expression using an *E. coli*-based IVTT expression kit lysate. All constructs were expressed via IVTT in 96-well PCR plate format and analyzed via SDS-PAGE in reducing and non-reducing conditions to confirm expression and molecular weight, and to evaluate cysteine bond formation. With the exception of non-optimized constructs, TMR-Halo ligand-labeled expression products were easily detected for all constructs at the expected molecular weight (**Figure 3**). However, all scFv constructs appeared to produce two distinct expression products. Because both products are also visible in reducing conditions, indicating these are not two different disulfide-bonded species, and because there is no known glycosylation machinery present in the lysate kit, it is likely that a second start site is being used for translation initiation. Interestingly, no additional expression products are observed for equivalents produced with human lysate, despite having the same amino acid sequence (data not shown).

Table 1: List of scFv and VHH constructs tested

Single Chain Antibody	References
Anti-Interluekin-6 (IL-6) (sirukumab) scFv	[14,15]
Anti-Human Serum Albumin (HSA) scFv	[16]
Anti-Tumor Necrosis Factor alpha (TNFa) VHH	[17]
Anti-Human Epidermal Growth Factor Receptor 2 (HER2) VHH	[13,18]
Anti-p53 scFv	[19]
Anti- Carcinoembryonic Antigen (CEA) scFv	[20]
Anti-EGFR (panitumumab) scFv	[21]

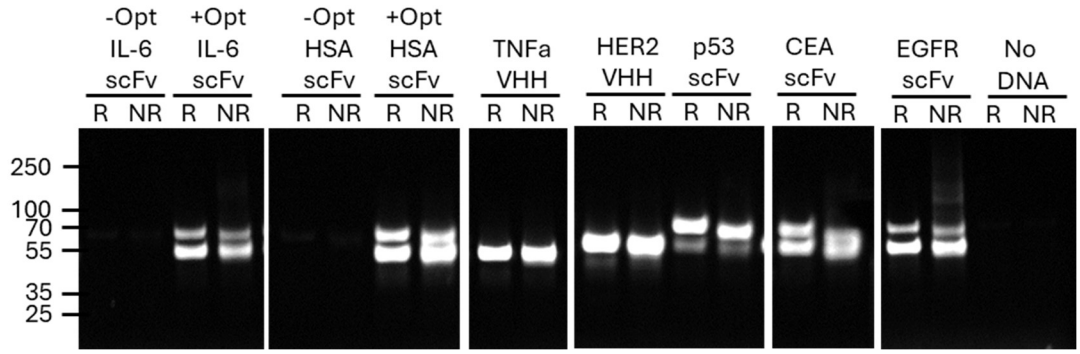

Figure 3: **SDS-PAGE analysis of C-Terminal HaloTagged scFvs and VHH expressed using *E. coli* lysate.** All expressed constructs were first covalently labeled with fluorescent Halo ligand then analyzed in reducing (R) and non-reducing (NR) conditions. A subset of constructs were expressed before (-Opt) and after (+Opt) optimization.

Analysis of constructs synthesized with or without optimization

Constructs for expression of scFvs in *E. coli* IVT systems were first designed based on a simple T7 Promoter-RBS-Gene-HaloTag-T7 Terminator structure. Sequences were taken directly from literature and converted to scFv format as required, with no optimization performed on linker length, sequence, or other structural considerations. A standard linker $(Gly_4Ser)_3$ was used for all scFv constructs tested. These scFv constructs yielded protein in low quantities, but still produced positive binding results when assayed against the scFv targets via fluorescent assay. Further optimization of constructs and expression conditions yielded at least an 8-fold higher expression of each construct and a corresponding higher level of target antigen bound by each scFv (**Figure 4**).

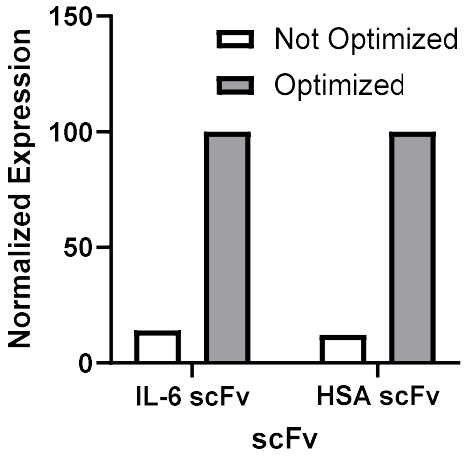

Figure 4: Optimization significantly improves expression levels of constructs expressed. Expression of IL-6 and HSA scFv constructs before and after optimization, normalized to optimized expression.

Confirmation of antigen target binding

ScFv and VHH HaloTag fusions were assessed for binding and specificity for their target antigens in a fluorescent sandwich assay. Antigens bound their corresponding single chain antibodies at various levels but each scFv or VHH showed high specificity for its target compared to all other antigens tested (**Figure 5**). As expected, little to no signal was observed for the scFv or VHH constructs when antigen was omitted as a negative control (**Figure 5A**), nor when the incorrect antigen and corresponding detection antibody was used (**Figure 5B**), confirming specificity. As expected, higher expression of the protein of interest following optimization also improved the total binding signal observed of target antigen.

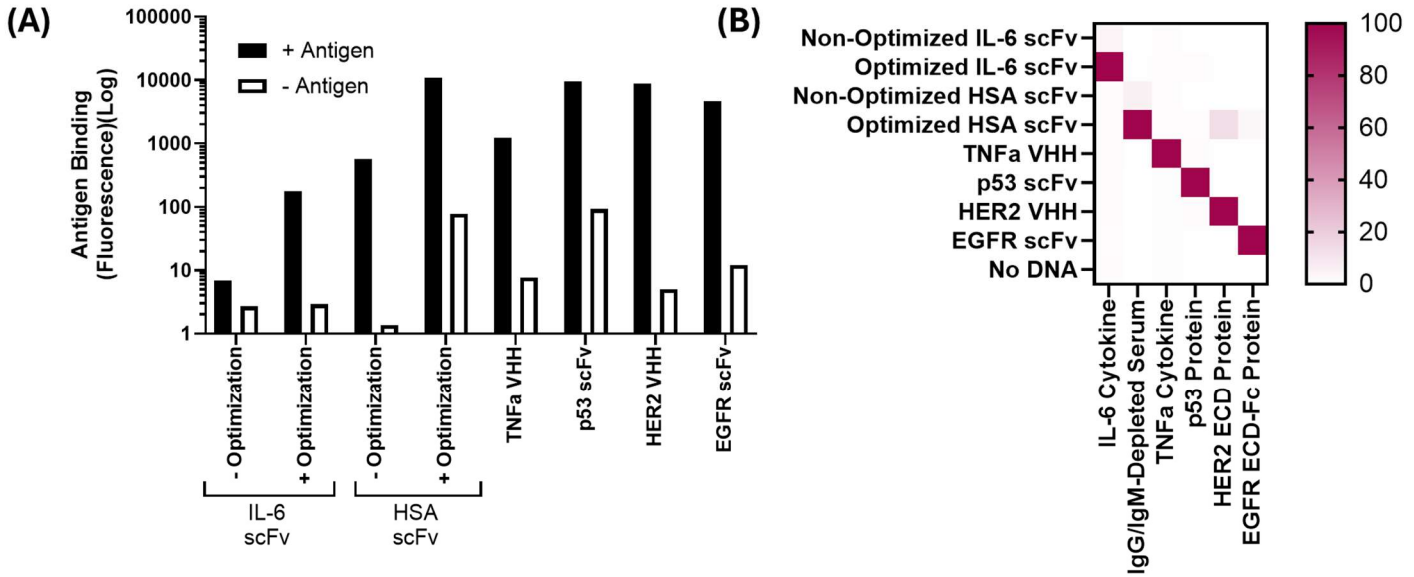

Figure 5: **Fluorescent-based analysis of single chain antibody constructs binding to target antigen.** C-terminal HaloTagged constructs were covalently linked to a glass surface via Halo ligand and incubated with (**A**) their target antigen (+Antigen) or PBST (-Antigen), or (**B**) all constructs were individually incubated with all antigens used in the assay. Antigens were detected via fluorescence using primary and secondary (if applicable) antibodies. A subset of constructs were expressed before (-Optimization) and after (+Optimization) optimization. IgG/IgM-Depleted Serum was used as the analyte for HSA.

Expression and capture of single chain antibodies on multiplexed SPOC SPR biosensors

High density protein biosensors were prepared for sc-antibody evaluation from nanowell slides printed with DNA encoding constructs designed for expression of sc-antibodies. ScFvs and VHHs expressed using an *E. coli* IVTT kit resulted in high levels (>200 RU) of protein captured on the surface, as measured with anti-HaloTag antibody (**Figure 6**). Recombinant protein antigens matching each of the tested scFv or VHH constructs were flowed over the SPR sensor surface and binding levels and kinetics were measured. Multiple single chain antibodies, both in scFv and VHH formats (anti-p53 scFv, anti-HSA scFv, anti-EGFR scFv, anti-CEA scFv, TNFα VHH, and HER2 VHH), were found to bind their target antigen at very high levels in a label-free format (**Figure 7A**). Sandwich antibody detection with antigen-specific antibodies for the target antigen were subsequently flowed across the sensor surface and confirmed the presence and specificity of the antigen for its antibody, and further increased the signal of IL-6 binding (**Figure 7C**). Specificity of the single chain antibodies and the secondary antibodies for cognate antigens was found to be very high (**Figure 7B, D**).

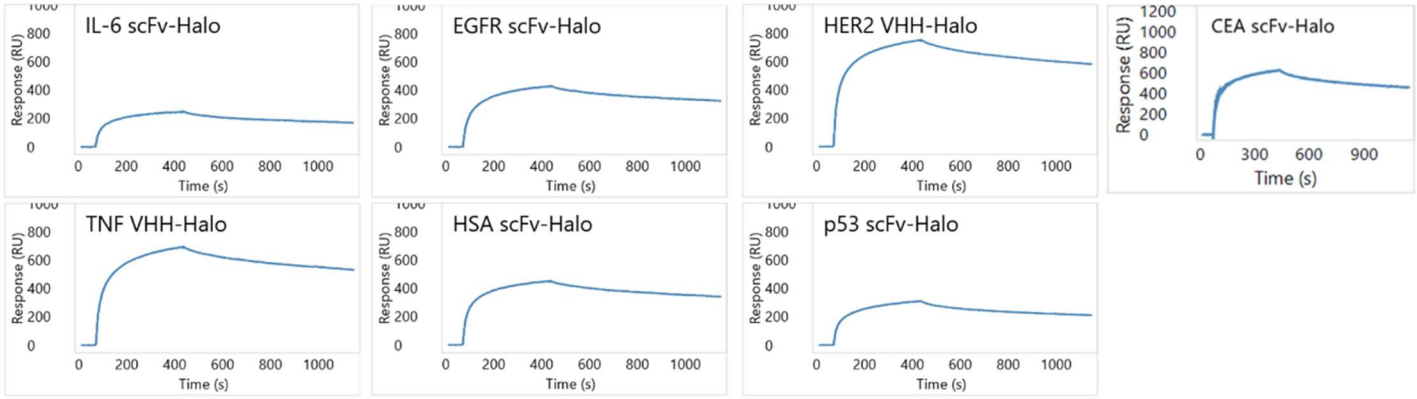

Figure 6. Confirmation of capture of scFv and VHH proteins with C-terminal HaloTag on SPOC biosensor. Capture levels on the biosensor of single chain antibodies expressed using a *E. coli* IVTT lysate were validated via anti-HaloTag antibody via SPR.

Affinity calculations from TNFα and HER2 VHH

Two constructs (TNFα and HER2 VHH) were chosen for full kinetic analysis. Kinetics were measured on SPOC SPR biosensors in duplicate (spot 1 and 2) by flowing recombinant antigen at multiple concentrations over the sensor surface while collecting kinetic data. Injecting TNFα over the biosensor in increasing concentration from 28 pM to 20 nM using 7 dilutions total resulted in an estimated affinity (K_D) of < 49 pM (**Figure 8A**). This is about 10-fold higher than the previously reported affinity of 540 pM for this VHH[17]. Due to the very high affinity of TNFα for the TNFα VHH, this affinity constant is only an initial estimate. This is because limited to no dissociation of bound TNFα was observed during the 30 minute dissociation window. Kinetics measured over a significantly longer dissociation window will be required for more accurate calculation of K_D, and will be performed prior to the submission to a peer review journal. The affinity constant for HER2 binding to the HER2 VHH was calculated to be 11.5 nM using an increasing 5-step titration of HER2 antigen from 1.8 nM to 150 nM (**Figure 8B**). This is similar to the reported K_D of 4 nM in literature for this VHH.

Design of single amino acid paratope mutations of HER2 VHH

Due to the clinical significance of HER2 therapeutic antibodies, the HER2 VHH was chosen for mutational analysis of the CDR regions that make up the paratope (antigen binding region) as a demonstration of SPOC biosensor utility in affinity maturation campaigns. Using data from Mitchell and Colwell[22] for manual CDR assignment and automated confirmation via INDI[23], CDR 1-3 were identified (**Figure 9A**) and each amino acid within the CDRs was individually mutated to alanine (substitution to a neutral, non-polar amino acid), aspartate (substitution to a negatively charged amino acid), lysine (substitution to a basic, positively charged amino acid), or serine (substitution to a neutral, polar amino acid), resulting in a total of 92 variants (**Figure 9B**). The DNA sequence was kept consistent except for mutations to ensure codon bias did not confound expression. The same codon was used within each amino acid substitution. Each variant was designed with a C-terminal HaloTag for covalent binding to the sensor.

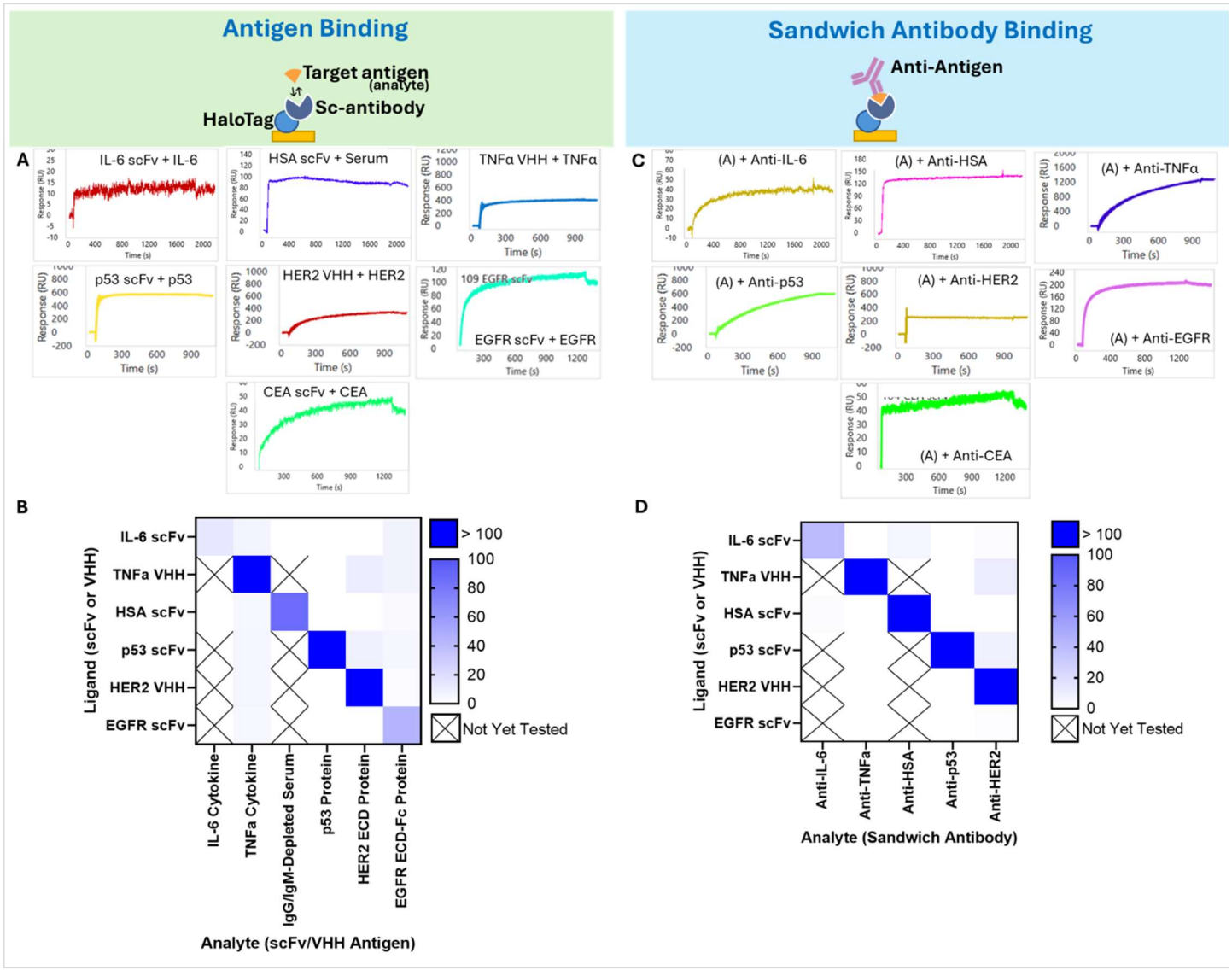

Figure 7. Analysis of scFv and VHH proteins on SPOC biosensor binding to antigen targets in comparison to non-targets. Antigen targets of the scFv and VHH proteins were analyzed for specific binding against all scFv and VHH simultaneously using a SPOC SPR biosensor. Binding traces to each cognate single chain antibody are shown in **(A)**, while maximum RU signal measured against all constructs at the end of the association phase (R_{Max}) is displayed in **(B)**. Binding traces of sandwich antibodies against each antigen, measured after flowing the antigen across the sensor, were collected and are shown in **(C)**, while the R_{Max} for each is shown in **(D)**. IgG/IgM-Depleted Serum was used as the analyte for HSA. X indicates selectivity data was not collected as part of this data set.

A

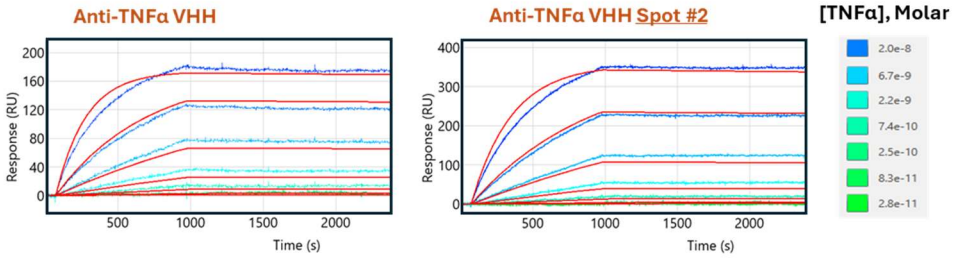

Anti-TNFα VHH	k_a ($M^{-1}s^{-1}$)	k_d (s^{-1})	K_D (pM)
#1	2.4e5	1.0e-5	≤42
#2	1.8e5	1.0e-5	≤56
		Avg K_D (pM):	**≤49**

B

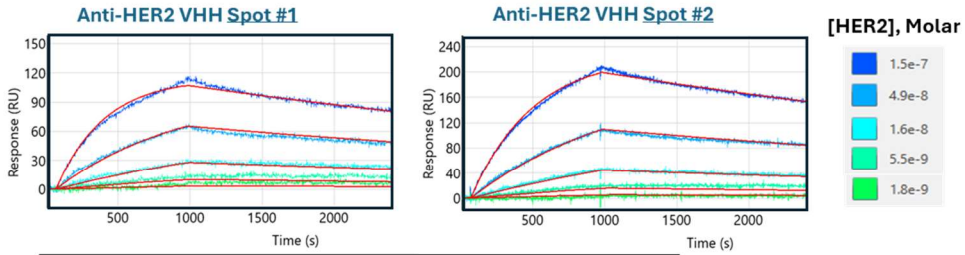

*Anti-HER2 VHH	k_a ($M^{-1}s^{-1}$)	k_d (s^{-1})	K_D (nM)
#1	1.9e4	2.0e-4	10
#2	1.5e4	1.8e-4	13
		Avg K_D (nM):	**11.5**

*Affinity of the Her2 Nanobody in literature reported to be K_D = 4.0 nM.

Figure 8. Kinetic analysis of TNFα and HER2 VHH constructs via SPR. Affinity constants for interactions between anti-TNFα VHH and TNFα were calculated from a titration of TNFα binding to the SPOC SPR sensor **(A)**. Regenerative conditions were used between TNFα injections due to high affinity of the interaction. However, lack of observed dissociation during the 20-minute window of the dissociation phase (data not shown) indicates that the affinity measured is an approximation of the real value, and disassociation measurements over significantly longer periods will be needed for accurate pM affinity calculation. The affinity constant for the interaction between anti-HER2 VHH with recombinant HER2 **(B)** was calculated from a titration of HER2 extracellular domain (ECD) binding using non-regenerative conditions. Kinetic measurements were averaged over the duplicate spots (1 and 2) for both VHH constructs.

A

MQVQLQESGGGSVQAGGSLKLTCAASGYIFNSCGMGWYR

CDR 1 (27-34)

QSPGRERELVSRISGDGDTWHKESVKGRFTISQDNVKKTLYL

CDR 2 (52-58)

QMNSLKPEDTAVYFCAVCYNLETYWGQGTQVTVSS

CDR 3 (97-105)

B

Alanine Mutants (Neutral, non-polar)		Aspartate Mutants (Acidic)		Lysine Mutants (Basic)		Serine Mutants (Neutral polar)	
G27A	G56A	G27D	G56D	G27K	G56K	G27S	G56S
Y28A	D57A	Y28D	T58D	Y28K	D57K	Y28S	D57S
I29A	T58A	I29D	A97D	I29K	T58K	I29S	T58S
F30A	V98A	F30D	V98D	F30K	A97K	F30S	A97S
N31A	C99A	N31D	C99D	N31K	V98K	N31S	V98S
S32A	Y100A	S32D	Y100D	S32K	C99K	C33S	C99S
C33A	N101A	C33D	N101D	C33K	Y100K	G34S	Y100S
G34A	L102A	G34D	L102D	G34K	N101K	I52S	N101S
I52A	E103A	I52D	E103D	I52K	L102K	S53S	L102S
S53A	T104A	S53D	T104D	S53K	E103K	G54S	E103S
G54A	Y105A	G54D	Y105D	G54K	T104K	D55S	T104S
D55A				D55K	Y105K		Y105S

Figure 9. **HER2 VHH (2Rs15d) wildtype sequence and resulting substitutions used in the mutation study.** The sequence and identified CDRs of HER2 VHH (2Rs15d) **(A)**. CDRs are highlighted in yellow and amino acid positions indicated for each. CDR amino acid substitutions to alanine, aspartate, lysine, and serine were designed into the constructs, resulting in 92 variants as shown in **(B)**.

Analysis of HER2 VHH CDR mutagenesis

SPOC biosensor chips with an sc-antibody library comprising mutated CDR variants were prepared from nanowell slides printed with DNA encoding constructs described above, and expressed using *E. coli* IVTT lysate. Recombinant HER2 extracellular domain (ECD) was used as the analyte to measure binding properties of each mutant (**Figure 10** and **Supplementary Table 1**). Calculation of affinity of wildtype/non-mutated HER2 VHH was consistently measured to be 30 nM ± 4.5 nM from three individual spots. The averaged values from these spots were used for comparison to mutants (**Figures 11-13**). Mutating Y105 to any amino acid resulted in a lower K_D (higher nM), while substitution of D55K resulted in the lowest K_D at 123 nM, ~4 times lower than WT. Altering C33 to any amino acid other than serine ablated binding below the defined detection limit, suggesting this is a critical paratope residue. Alternatively, changing Y28 to any amino acid had no significant effect on the K_D compared to WT, while N101D resulted in the highest affinity binder at 21 nM, though only a modest improvement over WT. Analysis of the dissociation rate alone was also performed to most accurately evaluate characteristics of the off-rate (**Supplementary Table 2**). For variants with an improved off-rate compared to wildtype (n=12), 75% were due to substitution with a charged amino acid, and all but one of these were located in CDR-2 or -3 (Y28K, G54K, G56D, T58K, T58D, N101K, L102K, L102D, T104D). A dissociation rate of 5.7e-5/s was measured for L102K, similar to a Trastuzumab scFv (kd 5.1e-5/s, data not shown). Higher resolution sensorgrams are shown for two variants (N101K and G54D) with low dissociation and high signal for comparison to wildtype (**Figure14**).

Figure 10. **Sensorgrams showing HER2 ECD titration kinetics for each of the 92 HER2 VHH mutant.** Titration was performed using non-regenerative conditions with increasing concentrations of HER2 ECD (1.65 nM, 4.96 nM, 14.9 nM, 44.7 nM, 134 nM, 402 nM), with all injections overlayed onto a single sensorgram. The red lines indicate the kinetic model curve fits to underlying data plots.

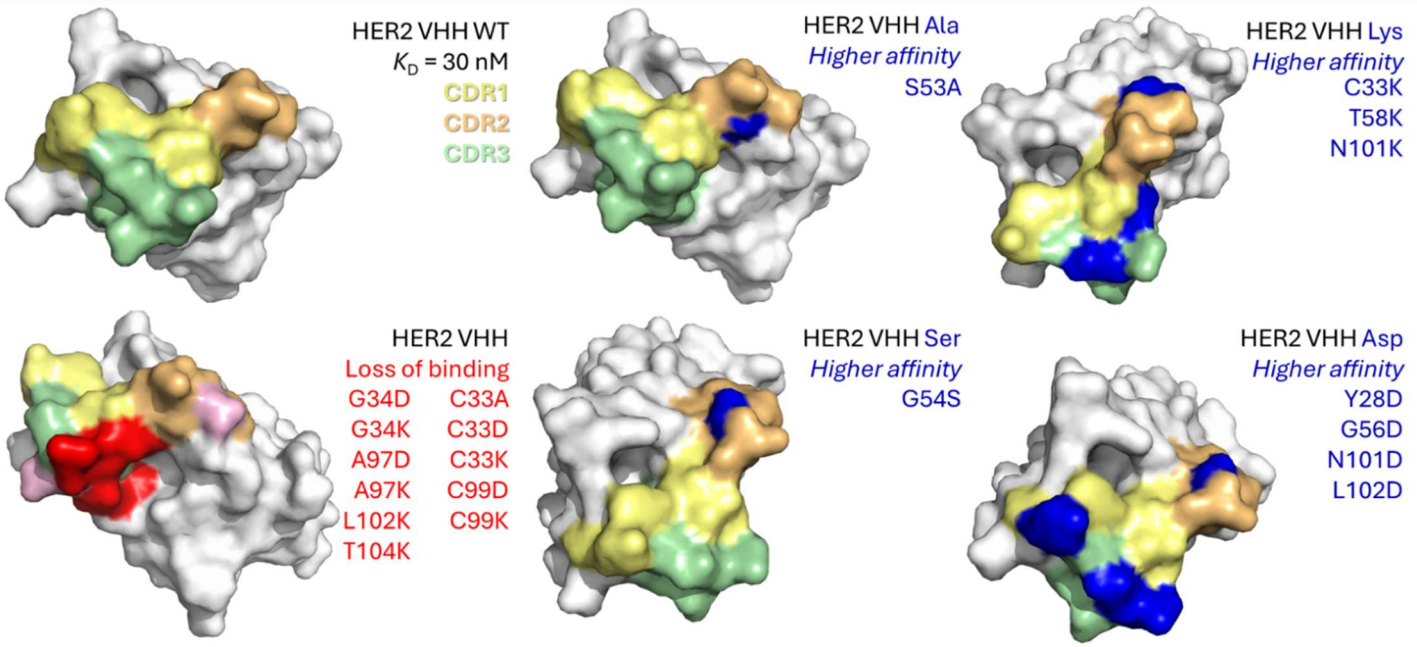

Figure 11. Visualization of residues that resulted in loss of binding or higher affinity upon substitution, in comparison to wildtype. CDRs 1, 2, and 3 are denoted in light yellow, light orange, and light green, respectively. Residues which produced higher affinity upon substitution are summarized visually in blue for each amino acid substitute (alanine, Ala; lysine, Lys; serine, Ser; aspartate, Asp) and specific substitutions are noted for each. Residues which resulted in loss of binding (red) or lower affinity 3-times or greater compared to wildtype (pink) are visualized in the lower left corner, with specific substitutions that resulted in loss of binding noted for each.

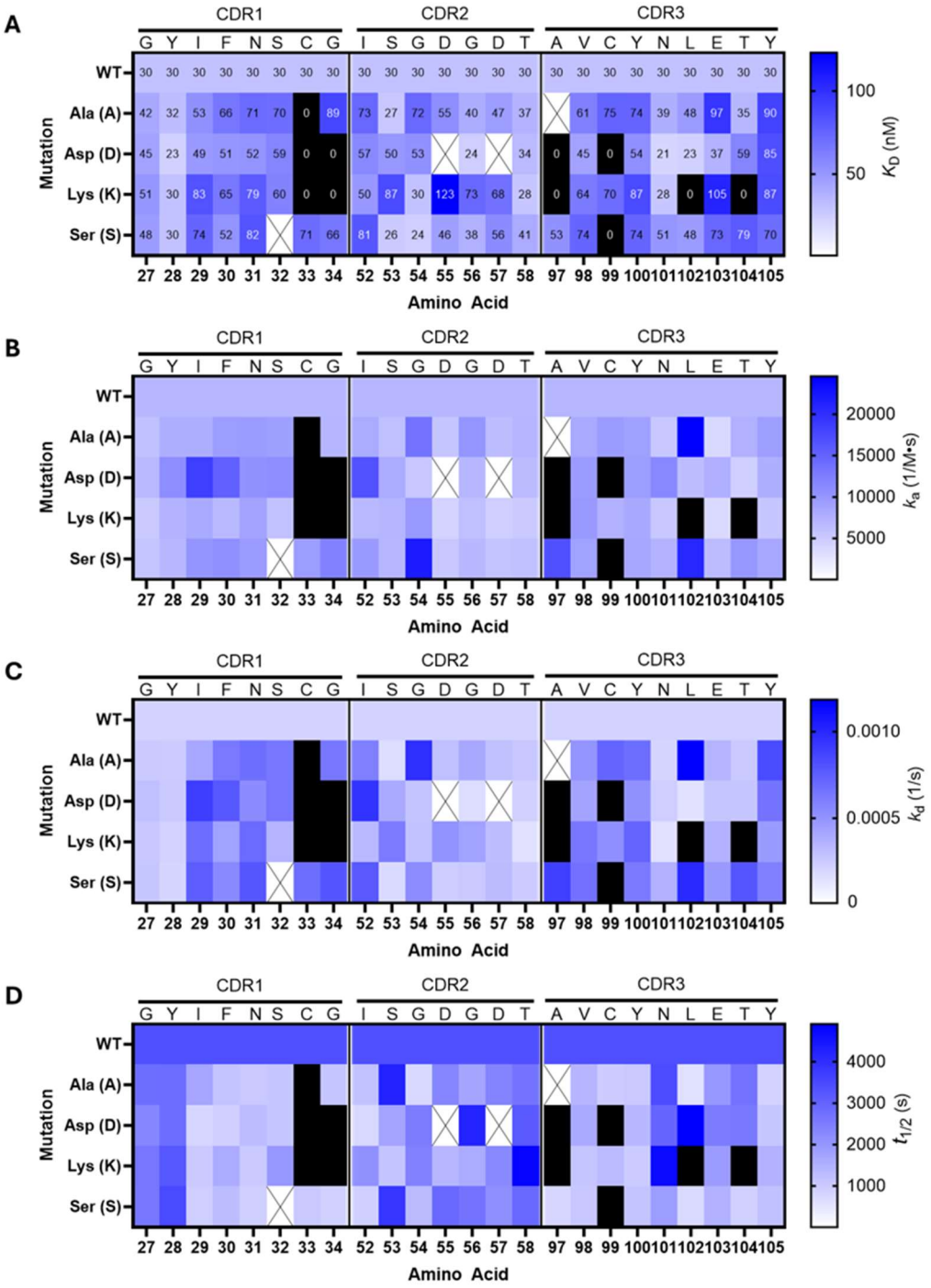

Figure 12. Heat maps visualizing kinetic binding data of the HER2 mutants. Affinity constant K_D **(A)**, on-rate k_a **(B)**, off-rate k_d **(C)**, and $t_{1/2}$ **(D)** is shown. White boxes marked with X indicate the substitution is the same amino acid as wildtype and thus were not produced/duplicated. Black boxes indicate no binding was observed as defined by highest signal at 400 nM HER2 injection resulting in response < 40 RU (~10% of the highest signal observed). Bar graphs of this data are shown in **Figure 13**.

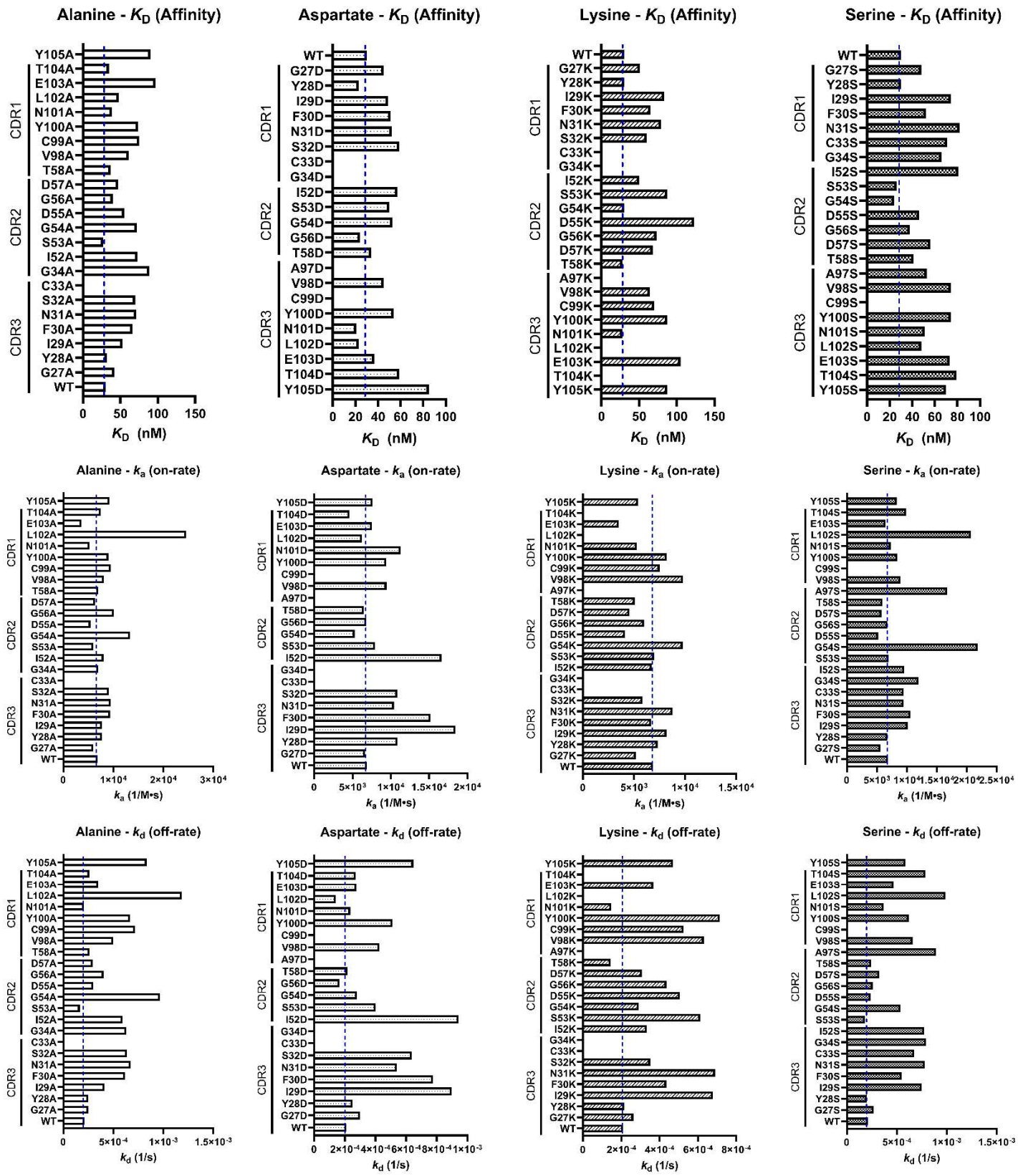

Figure 13. Bar graphs showing kinetic data obtained following a binding study of HER2 ECD against HER2 VHH mutants using a titration of HER2 ECD, organized by CDR and kinetic parameter. Affinity constant K_D for each amino acid substitution is shown in the top row, on-rate k_a is shown in the middle row, and off-rate k_d is shown in the bottom row. Missing bars indicate no binding was observed as defined by highest signal at 400 nM HER2 injection resulting in response < 40 RU (~10% of the highest signal observed).

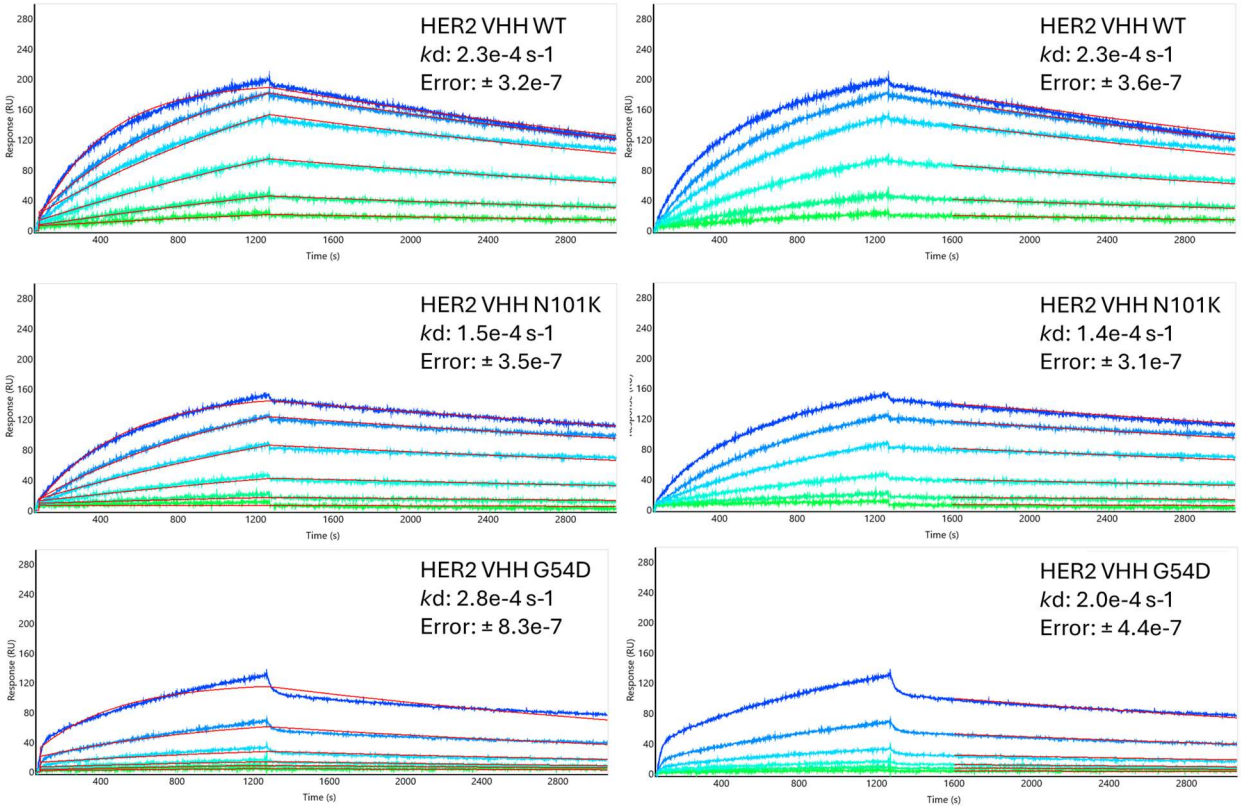

Figure 14. Select sensorgrams showing mutants with higher affinity compared to WT sequence. Left: Affinity curves (red) fitted to entire curve; Right: Curves fitted only for the dissociation (red).

Analysis of affinity of HER2 ECD for HER2 VHH produced from a titration of DNA encoding HER2 VHH

To determine whether evaluated kinetic parameters were dependent on the quantitative amounts of the mutated protein spots across the SPR chip, as each of the protein mutants may express at different levels, we performed an experiment where we titrated the printed amount of DNA encoding WT HER2 VHH into nanowells. We observed that although the magnitude of WT HER2 ECD binding signal increased with printed DNA concentration (peaking between 75-100 ng/μL), the evaluated affinity remained effectively the same. The result confirms that kinetics evaluated for different VHH variants is independent of any variant specific changes in proteins expression levels, over a certain cutoff. This shows that affinity is consistent and independent of levels or variation in protein quantities captured at each spot on the SPR biosensors. Affinity values for HER2 ECD binding to HER2 VHH (wildtype) expressed from DNA printed at 25, 33, 50, 75, and 100 ng/μL were measured to be 30 nM, 30 nM, 35 nM, 34 nM, and 30 nM, respectively, for an average of 31.8 nM ± 2.95 nM (**Figure 15**).

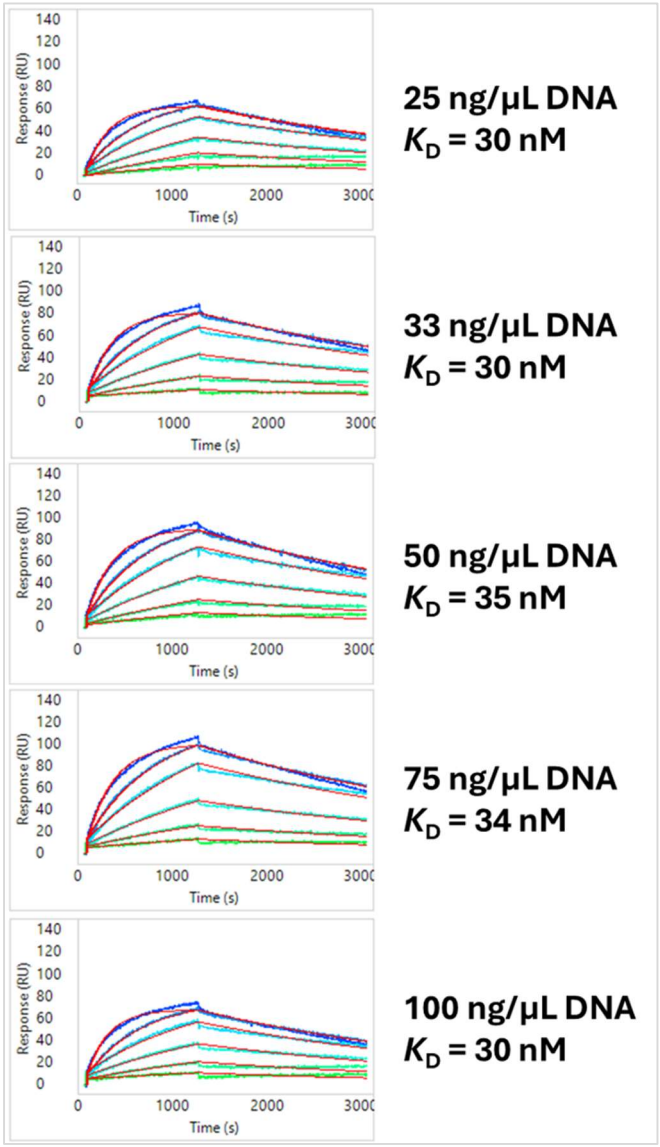

Figure 15. Varying input DNA concentration results in similar affinities for expressed protein. DNA encoding HER2 VHH wildtype was titrated during the nanowell printing process and the resulting protein expressed and captured onto the SPOC sensor was evaluated for binding with HER2 ECD.

Discussion

We have previously described a highly multiplexed method for measuring the kinetics of hundreds to thousands of protein interactions on a single biosensor using cell-free expression and high throughput SPR[12]. Here, we describe a new application of the SPOC platform demonstrating the production and testing of single chain antibodies via *in situ* cell-free expression and capture-purification onto SPR biosensors, with a use-case application of mutational scanning of an anti-HER2 VHH paratope.

For the development of this application, fluorescence-based assays were used as an initial test to validate antibody-target binding due to the ability to control a matrix of factors at one time for optimization of dilutions, buffers, and choice of detection antibody with high sensitivity. Following this, a set of sc-antibody molecules were tested using a SPOC chip on a custom Carterra SPR instrument to determine if scFv and VHH constructs produced in cell-free systems are functional and bind to respective targets with high specificity. This facilitates characterizing on-chip sc-antibody selectivity with significantly higher throughput, and to collect kinetic measurements of antigen binding for in-depth characterization and affinity ranking.

This paper demonstrates that the SPOC Protein Nano Factory (PNF) system produces functional single chain antibodies in the two forms tested directly on SPR biosensors: scFvs derived from full-length antibodies and single-domain antibody VHH, also commonly known as nanobodies. Two versions of a select few of the same scFvs were ultimately expressed using an *E. coli*-based kit. The first set of *E. coli* scFvs (non-optimized) produced functional antibody molecules capable of binding target antigen, but expression was low. For the second set of scFvs produced in *E. coli*, DNA construct and experimental condition optimization was performed, which resulted in 8-fold more protein on average (**Figure 2**). These optimizations produced scFvs that bound highly detectable target antigen on SPOC chips via SPR (**Figure 5**).

All subsequent *E. coli* scFvs and VHH constructs were synthesized post-optimization and their expression products were tested on SPOC biosensors. Expressed protein was confirmed to be present on the sensor at readily detectable levels as measured via anti-HaloTag antibody. It was immediately clear that 4 scFvs (targeting HSA, EGFR, p53, and HSA) and 2 VHH (targeting TNFa and HER2) bound their label-free target antigen at high levels at first assay with no additional optimization of SPR or expression parameters required. These constructs correlated well with previously reported affinity, with these immediately detectable antigens binding to constructs with low to sub-nanomolar affinity.

The constructs tested here had sequences taken directly from literature and were converted to scFvs using a single common linker of $(Gly_4Ser)_3$, without experimenting with multiple linker formats or other scFv components or scaffolds. We have also tested IFNγ, CA15.3, TNFa, and other HER2 scFv constructs using this common linker. CA15.3 and TNFa scFv have shown no binding thus far in this single-shot testing, while IFNg and Trastuzumab-derived HER2 scFv were shown to be capable of binding antigen (data not shown), though selectivity data is pending. Traditionally, scFvs are designed in the format of V_H-$(Gly_4Ser)_3$-V_L, as the most characterized and preferred linker format. However, given the precise scaffolding and folding requirements of scFvs, quite often this requires further optimization with different linker scaffolds if the initial format results in misfolding or aggregation, with no binding of target. Researchers often evaluate different linker lengths, different linker types, switching the order of the V_H and V_L, moving a purification or expression tag from one terminus to another, etc. We plan to test any non-functional scFv constructs with alternative linker designs and other formats in the future.

From these immediately functional constructs, two VHH were further analyzed to calculate affinity and limit of detection via injection of a titration of antigen. For the TNFα VHH, an approximate affinity of <49 pM was calculated, nearly 10-fold higher than the reported affinity of 540 pM for this VHH[17]. However accurate kinetics could not be measured due to the apparent lack of antigen dissociation over the 20 minute measurement window, used in this study. Further studies need to be performed with a significantly longer dissociation time, to accurately measure dissociation constant and evaluate affinity, and will be done prior to submission of paper to a peer review journal.

Furthermore, when using SPR biosensing to characterize kinetic parameters of very high affinity binders (picomolar to femtomolar affinities), we have the option of using the "chaser assay" method to accurately characterize ultra-low-dissociation-rate binding events measured by SPR instrument on SPOC chips. Used in the field of enzymology and more recently described in detail for application to SPR biosensing methodology by Quinn et al[24], this method uses a "chaser probe" to measure the fraction of free binding sites on the ligand epitope of interest after an acceptable dissociation time (minutes-hours versus many hours-days), resulting in high resolution readout at very high affinity. For the HER2 VHH, the measured affinity was more accurate due to measurable dissociation of the recombinant HER2 extracellular domain over a 20 minute window. This affinity was calculated to be 11.5 nM in this first study, very close to the previously reported affinity for this VHH of 4 nM[18].

As demonstration for use of the SPOC technology in drug development, we created a panel of paratope mutants of the HER2 VHH and measured the binding characteristics of HER2 to each mutant simultaneously on a single chip for direct comparison to one another. By mutating each amino acid individually to alanine within the three complementarity determining regions, it can be determined which amino acid side chains are critical for antigen binding. Similarly, by mutating the same residues individually to aspartate (acidic), lysine (basic), or serine (polar), we can determine if changing the side chain properties improves or reduces antigen binding. We found that several mutants improved overall affinity, with several improving the off-rate, though some mutants improved affinity by increasing the on-rate. Nearly all improvements in affinity were made by substitution of an uncharged amino acid with a charged amino acid.

During analysis of the kinetic data from the HER2 VHH mutant library, we found that certain HER2 VHH variants produced binding curves that deviated from the standard 1:1 binding model used for curve fitting (either due to presence of HER2 dimers or other factors that could have introduced kinetic heterogeneity). To more accurately estimate off-rates, a follow on analysis with the 1:1 binding model to the dissociation phase alone was performed. This analysis resulted in a more accurate fit of the dissociation kinetic curve for better comparison between mutants. As k_d is known to be the primary driver of the overall affinity of a molecule, especially when stronger binding is desired, an accurate comparison of this constant is required. It was noted that one particular variant, L102K, resulted in a very low dissociation (k_d = 5.7e-5/s), which was comparable to a trastuzumab (anti-HER2) scFv (k_d = 5.1e-5/s) present on the same sensor (data not shown). The variant with the second lowest dissociation rate was notably L102D (k_d = 1.1e-5/s), indicating this particular residue may be mutated for further improvement of k_d. Using data-trained AI-driven models for iterative design on more optimal sequences, 10 – 100x improvements in affinity via modulation of critical amino acids becomes possible.

There was a notable difference between the first measured affinity of HER2 ECD for HER2 VHH (11.5 nM) and the affinity measured for wildtype replicates in the follow-on second study that included mutation variants (30 nM). Though the affinities we report are lower than the original report of 4 nM, it well-known that the variation between instruments, especially those produced by different manufacturers, can be as high as 10-fold different[25,26]. More pertinently, there was one main difference between the first and the second study that may account for the 3-fold difference observed between the two affinities in this study. Of critical difference was the analyte used; though the HER2 ECD used was from the same batch, this recombinant protein was shipped in a buffer containing trehalose as a cryoprotectant which is known to cause a large bulk effect on the SPR signal, thus confounding data. To overcome the possibility of a bulk effect, we had to buffer exchange the protein into PBS to remove the trehalose and estimate the final protein concentration using absorbance at 260 nm. This method can be significantly inaccurate, especially for non-IgG proteins, but was used due to a supply shortage at the time of the study. Most critically, the analyte used for the first study was buffer exchanged separately from the second study; since both concentrations were merely an estimate, this is the most likely culprit for the differences in reported affinities between the two studies, as the analyte concentration directly impacts the affinity calculation. The authors would thus like to note that the correct concentration of each buffer exchanged batch will be measured via bicinchoninic acid (BCA) assay prior to submission to a peer review journal. Second, the process of buffer exchange may have resulted in differences in protein stability and/or dispersity, with the possibility of some species existing as different multimers if any aggregation occurred as a result of the exchange, or as inactive forms. It is notable,

however, that the second study included 8 replicates of the wildtype HER2 VHH (including the DNA titration in **Figure 11**), and had a low variation in affinity (30 nM ± 3.7 nM, n =8).

When using AI models for sc-antibody engineering, the SPOC platform addresses critical bottlenecks in the "build" and "test" phases by enabling the interrogation of thousands of nanobody candidates in a single assay. This facilitates the down-selection of the most promising candidates based on objective, high-affinity-resolution kinetic data. SPOC supports affinity maturation cycles by facilitating detailed characterization and engineering of antibody paratopes, enabling the design of variants with improved affinity, specificity, and selectivity. With its relatively low production cost, SPOC allows for comprehensive mutational scanning of antibody CDRs, substituting each position with all other amino acids (or a select subset) on a single SPR chip. This approach generates a complete, amino acid-level kinetic dataset to inform the "learn" phase and subsequent iterations of design-build-test-learn (DBTL) cycles. By performing this analysis on the same chip, SPOC ensures direct and confident comparisons of measurements between mutants and the wild-type baseline. Kinetic parameter ranking then enables the selection of binders tailored to specific therapeutic modalities or mechanisms of interest, such as those that bind with highest affinities, or that bind quickly (fast on-rate) at high levels, or that bind very tightly (slow off-rate), or a combination of these.

In conclusion, we have described for the first time a method for producing single chain antibodies on SPOC SPR biosensor chips via cell-free protein expression in a highly multiplexed format for label-free detection and characterization of target antigen binding. This method allows the user to simply use a DNA input for biosensor production of thousands of unique single chain antibody constructs, rather than expressing each construct of interest individually at in sufficient amounts followed by spotting or capturing onto a SPR biosensor chip for kinetic assay. SPOC can be applied to evaluating the affinities of antibodies produced via computational modeling to reduce downstream costs and increase the throughput of testing. For example, we demonstrated expression/production of a panel of 92 mutationally scanned variants from the CDR of HER2 VHH on one SPR biosensor, directly from DNA in an *E. coli* IVTT lysate. The SPOC SPR biosensor, meanwhile, has the capacity to interrogate up to 2,400 mutants, as reported previously. The result is the capability to collect and measure kinetic data at-scale at significantly lower cost per sequence than traditional recombinant production methods. This demonstrates a significant improvement to the ‘build’ and ‘test’ cycles required in traditional drug discovery, AI-enabled, and AI-driven workflows. Lastly, we demonstrated how a lead candidate can be mutationally scanned at low-cost and at high-throughput with kinetic measurements to support deep paratope characterization for subsequent affinity maturation campaigns, proposing the application of SPOC platform for iterative DBTL cycles to support traditional and AI drug discovery pipelines. The future goal for this application will be to fully incorporate SPOC analysis into AI drug discovery workstreams, to demonstrate how the improved ‘build’ and ‘test’ phases with increased sequence diversity testing capabilities, will improve the subsequent iterative ‘learn’ and ‘design’ phases and result in improved lead drug candidates, ultimately towards improving drug success rates.

Acknowledgements: We acknowledge partial funding support from NIH SBIR grant 1R44TR004297. We acknowledge Sharrol Bachas for helpful discussions on selecting the four diverse amino acids for CDR mutational scanning substitutions.

References

1. Sun, D., Gao, W., Hu, H. & Zhou, S. Why 90% of clinical drug development fails and how to improve it? *Acta Pharm Sin B* **12**, 3049–3062 (2022).

2. Smietana, K., Siatkowski, M. & Møller, M. Trends in clinical success rates. *Nat Rev Drug Discov* **15**, 379–380 (2016).

3. Barreto, K. *et al.* Next-generation sequencing-guided identification and reconstruction of antibody CDR combinations from phage selection outputs. *Nucleic Acids Res* **47**, e50–e50 (2019).

4. Yang, W. *et al.* Next-generation sequencing enables the discovery of more diverse positive clones from a phage-displayed antibody library. *Exp Mol Med* **49**, e308–e308 (2017).

5. Erasmus, M. F. *et al.* Insights into next generation sequencing guided antibody selection strategies. *Sci Rep* **13**, 18370 (2023).

6. Mejias-Gomez, O. *et al.* Deep mining of antibody phage-display selections using Oxford Nanopore Technologies and Dual Unique Molecular Identifiers. *N Biotechnol* **80**, 56–68 (2024).

7. Sun, X., Zhou, C., Xia, S. & Chen, X. Small molecule-nanobody conjugate induced proximity controls intracellular processes and modulates endogenous unligandable targets. *Nat Commun* **14**, 1635 (2023).

8. Scully, M. *et al.* Caplacizumab Treatment for Acquired Thrombotic Thrombocytopenic Purpura. *N Engl J Med* **380**, 335–346 (2019).

9. Martin, T. *et al.* Ciltacabtagene Autoleucel, an Anti–B-cell Maturation Antigen Chimeric Antigen Receptor T-Cell Therapy, for Relapsed/Refractory Multiple Myeloma: CARTITUDE-1 2-Year Follow-Up. *Journal of Clinical Oncology* **41**, 1265–1274 (2023).

10. Markham, A. Envafolimab: First Approval. *Drugs* **82**, 235–240 (2022).

11. Keam, S. J. Ozoralizumab: First Approval. *Drugs* **83**, 87–92 (2023).

12. *Novel Sensor Integrated Proteome on Chip (SPOC TM) Platform for Evaluating Kinetic Parameters of Protein Interactions in High Throughput*.

13. D'Huyvetter, M. *et al.* 131I-labeled Anti-HER2 Camelid sdAb as a Theranostic Tool in Cancer Treatment. *Clin Cancer Res* **23**, 6616–6628 (2017).

14. Xu, Z. *et al.* Pharmacokinetics, pharmacodynamics and safety of a human anti-IL-6 monoclonal antibody (sirukumab) in healthy subjects in a first-in-human study. *Br J Clin Pharmacol* **72**, 270–81 (2011).

15. Ehrenmann, F., Kaas, Q. & Lefranc, M. IMGT/2Dstructure-DB card for INN 9431 (sirukumab). *IMGT/3Dstructure-DB* https://www.imgt.org/3Dstructure-DB/cgi/details.cgi?pdbcode=9431 (2024).

16. Adams, R. *et al.* Extending the half-life of a fab fragment through generation of a humanized anti-human serum albumin Fv domain: An investigation into the correlation between affinity and serum half-life. *MAbs* **8**, 1336–1346 (2016).

17. Beirnaert, E. *et al.* Bivalent Llama Single-Domain Antibody Fragments against Tumor Necrosis Factor Have Picomolar Potencies due to Intramolecular Interactions. *Front Immunol* **8**, 867 (2017).

18. Vaneycken, I. *et al.* Preclinical screening of anti-HER2 nanobodies for molecular imaging of breast cancer. *The FASEB Journal* **25**, 2433–2446 (2011).

19. Caron de Fromentel, C. *et al.* Restoration of transcriptional activity of p53 mutants in human tumour cells by intracellular expression of anti-p53 single chain Fv fragments. *Oncogene* **18**, 551–7 (1999).

20. Boehm, M. K. *et al.* Crystal structure of the anti-(carcinoembryonic antigen) single-chain Fv antibody MFE-23 and a model for antigen binding based on intermolecular contacts. *Biochem J* **346 Pt 2**, 519–28 (2000).

21. Ehrenmann, F., Kaas, Q. & Lefranc, M. IMGT/3Dstructure-DB card for 5sx4 (panitumumab). *IMGT/3Dstructure-DB* https://www.imgt.org/3Dstructure-DB/cgi/details.cgi?pdbcode=5SX4 (2024).

22. Mitchell, L. S. & Colwell, L. J. Comparative analysis of nanobody sequence and structure data. *Proteins* **86**, 697–706 (2018).

23. Natural Antibody - NANOBODY Database. *http://research.naturalantibody.com/nanobodies* (2024).

24. Quinn, J. G., Pitts, K. E., Steffek, M. & Mulvihill, M. M. Determination of Affinity and Residence Time of Potent Drug-Target Complexes by Label-free Biosensing. *J Med Chem* **61**, 5154–5161 (2018).

25. Yang, D., Singh, A., Wu, H. & Kroe-Barrett, R. Determination of High-affinity Antibody-antigen Binding Kinetics Using Four Biosensor Platforms. *J Vis Exp* (2017) doi:10.3791/55659.

26. Katsamba, P. S. *et al.* Kinetic analysis of a high-affinity antibody/antigen interaction performed by multiple Biacore users. *Anal Biochem* **352**, 208–21 (2006).